THE JOURNAL OF PHYSICAL CHEMISTRY C

Article

pubs.acs.org/JPCC

# Morphology and Optical Response of Carbon Nanotubes Functionalized by Conjugated Polymers

Al'ona Furmanchuk,[†] Jerzy Leszczynski,[†] Sergei Tretiak,[‡] and Svetlana V. Kilina*[,§]

[†]Department of Chemistry and Biochemistry, Jackson State University, Jackson, Mississippi 39217, United States

[‡]Theoretical Division and Center for Integrated Nanothechnology, Los Alamos National Laboratory, Los Alamos, New Mexico 87545, United States

[§]Department of Chemistry and Biochemistry, North Dakota State University, Fargo, North Dakota 58108, United States

Supporting Information

**ABSTRACT:** Noncovalent functionalization of single wall carbon nanotubes (SWNTs) by biological and conjugated polymers promises significant improvements in their properties important for future nanotube-based optoelectronic and photovoltaic devices. Using a combination of molecular mechanics and quantum chemistry methods, we investigate how the deposition of poly-phenylene vinylene (PPV), a conjugated polymer, on the surface of selected SWNTs affects their morphology, as well as their electronic and optical properties. We found that the interaction between PPV and the nanotube is relatively weak (0.1−0.3 eV per repeat unit), and the most stable structures exhibit small coiling angles (≤20°) of PPV chains around the nanotube. PPV functionalization weakly affects optical excitations of the SWNT, resulting in slight red-shifts of the first and second optical bands of the nanotube. In contrast, the absorption spectra of PPV are strongly affected by specific conformational structures of the wrapped polymer. Our analysis identifies and explains a significant blue-shift of the excited energy and much broader line-width of the coiled PPV compared to that of the respective isolated polymer structures. These trends convey that signatures of polymer wrapping around SWNTs can be detected in experimental optical spectra of hybrid composites.

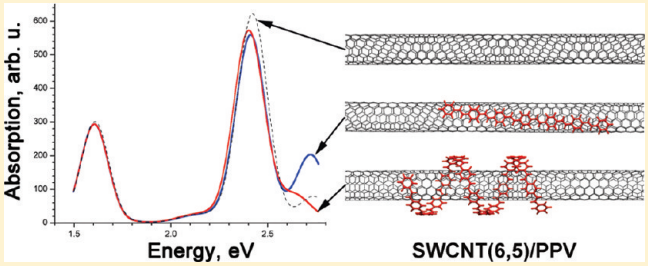


## INTRODUCTION

Quasi-one-dimensional nanostructures with unique optoelectronic properties, single-walled carbon nanotubes (SWNTs), have been known as promising materials for various applications, including field effect transistors,[1−3] light-emitting diodes,[4,5] solar cells,[6] and biosensors.[7−9] Compared to other systems, however, our progress in understanding and manipulating fundamental optoelectronic properties of nanotubes and designing subsequent practical applications is relatively slow. The challenge is that current methods of nanotube synthesis produce a wide range of nanotube geometries with different chiralities (characterized by different $(n,m)$ indices), which results in variations of their electronic and optical properties. In addition, strong van der Waals interactions between individual tubes result in the formation of bundles with significantly decreased solubility and low photoluminescence yield. These synthetic issues hinder practical implementation of nanotube-based materials at the industrial level. However, unbundling, purity and quality of nanotube samples, working characteristics, and manipulation of SWNT physical properties can all be significantly improved through selective chemical functionalization of SWNTs by small organic surfactants, polymers, and biomolecules.

Among available functional groups, one of the most promising compounds are organic semiconductors such as conjugated polymers. Conjugated polymers have a low manufacturing cost, improved scalability, and the potential to make lightweight and flexible devices. In addition, conjugated polymers are also versatile materials with strong carrier transport and useful optical properties. As such, development of novel hybrid materials based on SWNTs functionalized by conjugated polymers creates exciting opportunities for new functionalitities of these materials. For example, selective binding of nanotubes with different types of conjugated polymers provides a simple method of dispersing them in various organic solvents,[10−15] helps to decrease bundling,[16] and consequently improves optoelectronic properties.[17−21] The ability of some conjugated polymers to selectively interact with specific nanotube types in solution holds great promise for nondestructive separation of SWNTs with different chiralities.[22−26] SWNTs wrapped in polymers have demonstrated a photogating effect on charge transport amplifying current flow through the nanotube.[27] Furthermore, nanotube−polymer interactions can provide necessary conditions for ultrafast charge transfer from the polymer to the SWNT required for the efficient operation of photovoltaic devices.[28,29]

In addition to improved nanotube properties, hybrids also demonstrate enhancement of the wrapped conjugated poly-

**Received:** November 30, 2011
**Revised:** February 23, 2012
**Published:** February 28, 2012

mer's electro-optical properties. Thus, the addition of SWNTs to various types of conjugated polymers, such as poly[meta-phenylene vinylene-*co*-2,5-dioctoxy-para-phenylene vinylene] (PmPV),[30−32] poly-para-phenylene vinylene (PPV),[33] and poly[2-methoxy-5-(2-ethyl-hexyloxy)-1,4-phenylenevinylene] (MEH-PPV),[34] increases both the electrical conductivity and the lifetime of electroluminescence[35] and photoluminescence,[36] compared to the pristine polymer samples. This improvement and enhancement of specific properties of hybrids is controlled by nanotube−polymer interactions and their mutual morphologies. Typically, polymer functionalization of SWNTs has a noncovalent character, with the nanotube interacting weakly with the polymer via van der Waals forces or $\pi-\pi$ stacking.[37,38] In such hybrid materials, conjugated polymers are helically wrapped[39] or linearly adsorbed along the nanotube.[40] The geometrical features of the polymer−SWNT interface are important in determining the physical and electrical properties of the complex. It has been shown that the physical interactions of the SWNTs and polymers determine the low dispersion limit in solvents of nanotube−polymer hybrids.[41] Parallel assembly of polymers along the SWNTs results in self-assembled nanotubes in ordered ribbon-like structures.[42] Intimate heterojunction contacts and interfacial areas between the polymer and the nanotube play an important role in photoexcited dynamics of hybrids, including energy and charge transfer,[29] transport properties,[43] and photoluminescence.[21]

Despite the efforts of numerous studies in this area, an understanding of the inherent interface physics between adsorbed organic molecules and the nanotube surface is still limited. The problem originates from the challenge of resolving features associated with polymer−SWNT interactions, which do not have direct signatures in conventional spectroscopic techniques. As such, theoretical and computational methods could provide valuable insights into these issues and complement experimental investigations. So far, theoretical studies of the polymer-functionalized SWNTs have been mostly focused on the structural aspects of hybrids. For example, tube chirality selectivity[24,25] has been investigated using classical molecular dynamics[44−47] and Monte Carlo simulations.[48] Only a little effort has been done regarding simulations of optical properties of isolated oligomers with wrapped geometries as on a tube surface.[49]

In the present article, we perform a systematic theoretical investigation of morphology, electronic structure, and optical properties of SWNTs noncovalently functionalized by the PPV oligomer. While the majority of previous theoretical studies have been focused on the simulations of geometries of hybrids predicting either helical polymer wrapping[25,47,50] or parallel alignment depending on the flexibility of backbones,[44,45] here we address the question of how different PPV conformations on the nanotube surface affect the optical response of both components. We utilize a combination of the molecular mechanics approach, using the MM3 force field for finding stable geometries, and quantum chemistry techniques based on configuration interaction singles (CIS) coupled to the semiempirical ZINDO Hamiltonian for calculation of optical properties. We have found that PPV functionalization only slightly perturbs the nanotube structure, insignificantly red-shifting the first and second optical bands of SWNTs. In contrast, the adsorption spectra of PPV are strongly affected by its wrapping geometries, noticeably blue-shifting and broadening the spectra for the highly coiled PPV chains.

## METHODS

The systems considered in the present study consist of a PPV oligomer along with (6,5) and (8,0) nanotubes, representing a typical class of chiral and zigzag SWNTs, respectively. Ground state geometries of pristine (6,5) and (8,0) SWNTs of about 10 nm in length have been obtained by using the semiempirical AM1 Hamiltonian[51] as was described elsewhere.[52] In order to suppress dangling bonds and open the band gap in the finite size tubes, the ends have been capped by hydrogen atoms in the case of the (6,5) SWNT and by methylene groups for the (8,0) SWNTs, according to the procedure used in the previous studies.[52−54] It has also been shown[55] that such an approach can be successfully used for predictions of the ground and excited state properties of a variety of SWNTs. Here, AM1 optimized geometries of SWNTs have been used in all calculations

To get the final geometries of the tube−polymer composites, we have started with some initial wrapping angles of the polymer chain with respect to the tube surface. The hybrid systems have then been optimized to their energy minima (see Figure 1) using two different methods. For the first method,

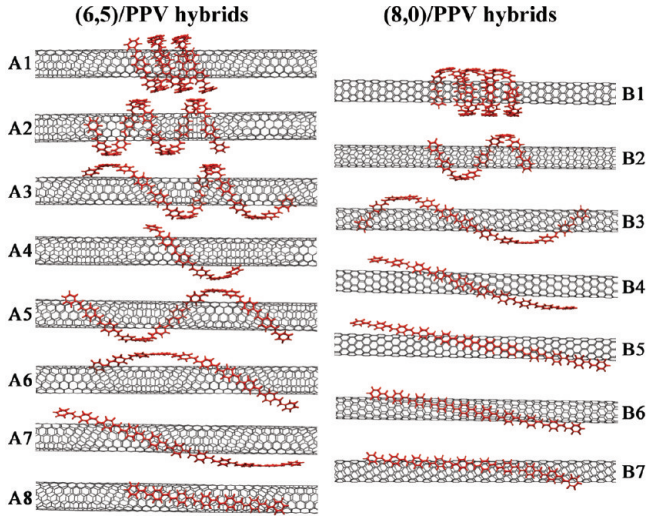


**Figure 1.** Structures of studied hybrid systems of PPV oligomers with the (6,5) nanotube (on the left) and the (8,0) nanotube (on the right). The labels of PPV/SWNT hybrids are used throughout the article.

we use a relatively long PPV oligomer consisting of 68 repeat units and allow all atoms of the polymer to freely move during geometry optimization. For the second approach, only central atoms of the short PPV oligomers of 10−20 units in size are permitted to move, while the oligomer ends have been fixed at certain positions from the tube surface (consistent with van der Waals distances) during optimization. The second approach allows us to apply approximate constraints on the polymer wrapping created by long chains, despite the actual small size of the systems. All optimization procedures of PPV oligomers wrapped around the nanotubes have been done using classical molecular dynamics, as implemented in the Tinker program.[56] MM3-2000 force-00000 field[57,58] parameters have been modified[59,60] to reproduce the AM1 geometry of the isolated PPV oligomer. On the basis of results of MM3 optimization, the binding energy between PPV and SWNT is calculated according to the standard definition: Energies of individually


dx.doi.org/10.1021/jp211541q | J. Phys. Chem. C 2012, 116, 6831−6840

optimized components (isolated PPV and isolated SWNT) are subtracted from the total energy of the optimized SWNT−PPV hybrid structure.

After the optimization step, the PPV oligomer sizes have been reduced so that the resulting hybrid PPV/SWNT structures do not exceed 1000 atoms. This corresponds to a tube length of about 10 nm and PPV oligomers of 6−22 repeat units in length depending on their wrapping angles, as illustrated in Figure 1. We use the following criteria for reducing the number of unit cells in final structures: (i) For tightly wrapped oligomers, we allow at least three turns of the PPV chain around the nanotube in order to model an effect of congregated units. (ii) To prevent edge effects, the oligomers coiled at small angles are shortened, so that they do not exceed the edges of the SWNTs. Thus, PPV oligomers are shorter in structures with small wrapping angles than in structures with tightly coiled oligomers.

The reduced final geometries have been utilized for analysis of the electronic structure and optical spectra of hybrid PPV−SWNT systems. The first 150 (for (6,5)/PPV) and 200 (for (8,0)/PPV) lowest excited-state energies and their respective oscillator strengths have been computed with the configuration interaction for singles (S-CIS) technique coupled to the intermediate neglect of the differential overlap/spectroscopy (INDO/S) model, as incorporated in the collective electronic oscillator (CEO) package.[61−63] To simulate the absorption spectra, an empirical Gaussian line width parameter of 0.01 eV has been chosen to address various broadening effects that occur under experimental conditions. Natural transition orbital (NTO) analysis[64] for selected excitations has been performed to analyze the properties of the electronic transitions in terms of orbitals. Since most of the excited states in the considered composites exhibit complex multiconfigurational character, the two most significant NTO pairs (electron and hole orbitals) are shown for each optical transition. The NTO analysis has been carried out using Gaussian 03 code[65] and the INDO/S-CIS model (the same as the CEO calculations) for all PPV/SWNT structures. The first 10 excited singlet states for isolated PPV oligomers have also been calculated and analyzed at the same level of theory.

## RESULTS AND DISCUSSION

**Wrapping Conformations and Binding Energies between PPV Chains and Nanotubes.** Selected structures of PPV oligomers differently coiled around (6,5) and (8,0) SWNTs are depicted in Figure 1. All hybrid structures are stabilized by $\pi-\pi$ interactions between PPV and the nanotube. By changing the wrapping angle for the initial configuration, we can limit the ability to form these $\pi-\pi$ interactions by a certain amount. At the same time, the structure of the PPV oligomer slightly adjusts itself to achieve the highest possible $\pi-\pi$ overlap between PPV and SWNTs for a particular coiling. In fact, not only PPV chains with strongly distorted helical structures but also oligomers with very small wrapping angles in hybrid structures demonstrate a slight deviation in carbon−carbon bond lengths compared to the isolated, ideal PPV chain (see Table S1 in the Supporting Information).

On average, PPV carbon−carbon double and single bonds in both types of hybrids are equal to 1.345 and 1.452 Å, respectively. Their difference, the so-called bond length alternation (BLA), is a critical structural parameter strongly coupled to the molecular electronic structure of conjugated polymers. The average BLA we found is 0.107 Å (±0.003−0.004 Å) in both hybrids. The largest BLA is observed for PPV chains with wrapping angles of ∼20° (A7 and B4 structures). Such an increase of the BLA value corresponds to a lower degree of conjugation in the oligomer coiled at 20°. Also, PPV wrapping around the nanotube results both in large variations of torsion angles between PPV units and in slight changes of carbon−carbon bond lengths in the phenyl rings (1.400 ± 0.003 Å) of the oligomer. The changes in carbon−carbon bond lengths in SWNTs due to PPV functionalization are negligible. No uniform relationship between PPV−SWNT distances and the conjugation degree of PPV oligomers has been observed in simulated hybrids. However, there is an expected tendency toward higher conjugation (small BLA) in the PPV for weakly interacting SWNT/PPV hybrids with PPV−SWNT spacing >3.4 Å. On the other hand, hybrids having very small PPV−SWNT distances <3.3 Å exhibit a significant decrease in conjugation (see Table S1 in the Supporting Information).

In all hybrids, the average spacing between the PPV oligomer and the nanotube varies from 3.27 to 3.61 Å, typically decreasing with the strength of the PPV−SWNT interaction; see Table 1. The most stable hybrid configurations exhibit the optimal polymer−tube distance of ∼3.3 Å, common for $\pi-\pi$ stacking, thus confirming the dominant mechanism of interaction between the nanotube and the PPV polymer is indeed through $\pi-\pi$ stacking. Note that the obtained binding energies (Table 1) are higher than typical $\pi-\pi$ interactions in a benzene dimer, which is 2.4 kcal/mol (∼0.11 eV) in the gas phase, as calculated by the coupled cluster theory (CCSD).[66] MM3 force filed calculations of binding energies between two benzene molecules result in 2.51 and 2.14 kcal/mol for parallel-displaced (one benzene molecule is shifted by one-half of a ring with respect to another molecule) and sandwich (the ring above the ring) structures, respectively. These values agree with those obtained by high-level *ab initio* theories. This agreement provides an indirect proof that MM3 calculations are reliable in predictions of $\pi-\pi$ interactions. Most likely, conjugation in both SWNT and PPV results in delocalization of orbitals over the entire system and overall increase in

**Table 1. Structural Characteristics (Average Values) and Binding Energies of PPV/SWNT Composites Obtained from MM3 Force Field Optimization**

| hybrid type | structure | wrapping angle (deg) | PPV−SWNT distance (Å) | number of units in PPV | $E_{bind}$/unit (eV) |
|---|---|---|---|---|---|
| PPV/(6,5) | A9 | 0.98 | 3.33 | 11 | −0.38 |
| | A8 | 5.25 | 3.34 | 7 | −0.36 |
| | A7 | 19.91 | 3.31 | 11 | −0.32 |
| | A6 | 27.93 | 3.43 | 10 | −0.29 |
| | A5 | 42.82 | 3.27 | 13 | −0.15 |
| | A4 | 48.77 | 3.46 | 6 | −0.13 |
| | A3 | 56.03 | 3.40 | 16 | −0.07 |
| | A2 | 70.28 | 3.53 | 17 | 0.16 |
| | A1 | 75.83 | 3.54 | 18 | −0.02 |
| PPV/(8,0) | B8 | 0.20 | 3.32 | 11 | −0.36 |
| | B7 | 7.23 | 3.33 | 10 | −0.35 |
| | B6 | 9.98 | 3.33 | 10 | −0.35 |
| | B5 | 11.24 | 3.36 | 12 | −0.34 |
| | B4 | 19.66 | 3.29 | 10 | −0.31 |
| | B3 | 34.37 | 3.40 | 13 | −0.20 |
| | B2 | 58.60 | 3.28 | 9 | 0.02 |
| | B1 | 72.77 | 3.61 | 22 | 0.10 |


dx.doi.org/10.1021/jp211541q | J. Phys. Chem. C 2012, 116, 6831−6840

SWNT−polymer binding, compared to isolated benzene−benzene interactions.

As can be seen from Figure 2, the more stable configurations of PPV/SWNT hybrids have PPV wrapping angles $\alpha < 30°$

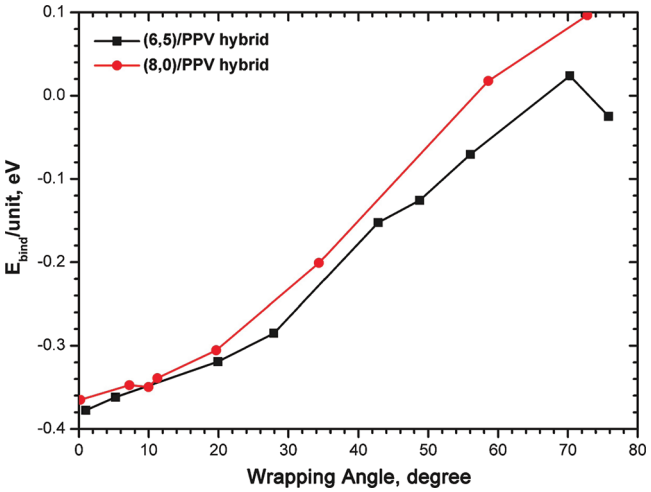


**Figure 2.** Binding energy per polymer repeat unit as a function of a wrapping angle for different PPV/SWNT hybrids. Configurations with small wrapping angles with respect to the nanotube axis are the most stable.

with absolute values of binding energies equal to 0.3−0.4 eV per polymer repeat unit (see Table 1). The most energetically favorable configuration corresponds to $\alpha \approx 0°$, when PPV is nearly parallel to the tube axis. However, the energy barrier between configurations with $\alpha \approx 0°$ and $5° \leq \alpha \leq 20°$ is very small, on the order of $kT$ (0.02−0.06 eV). Thus, thermal fluctuations might slightly distort the wrapping angles, so that different conformations with wrapping angles varying from 0 to 20° may be equally probable. For large wrapping angles $\alpha \geq 60°$, the hybrids are unstable, having binding energy $E_{bind} \approx 0$ eV or even $E_{bind} \geq 0$ eV for both (6,5) and (8,0) tubes.

The decrease in hybrid stability, when the PPV wrapping angle increases, originates from an interplay between $\pi-\pi$ stacking interactions and steric repulsion energies. While bending of PPV structures with small angles (<20°) negligibly affects the total energy of the oligomer (comparable to thermal fluctuations), bending of PPV chains into tightly coiled structures significantly destabilizes the energy of the oligomer by 0.1−0.4 eV. (Energy differences between the coiled oligomer and the same length linear fully optimized PPV are presented in Table S1 in the Supporting Information.) In composites, twisted and bended configurations can be partially stabilized by $\pi-\pi$ interactions between neighboring molecules, such as nanotubes in our case. However, wrapping of PPVs at large angles also leads to steric interactions and repulsion between coiled PPV loops. At large wrapping angles, the energy of such steric repulsions is so large that it cannot be compensated by $\pi-\pi$ interactions with nanotubes. Overall, our simulations predict stable PPV/SWNT configurations only with relatively small wrapping angles $\alpha \leq 20°$.

Helical wrapping of PPV on tube surfaces has been previously reported in the literature. Simulations based on molecular dynamics have predicted small coiling of conjugated polymers with stiff backbones, rather than a strictly linear alignment on a nanotube surface.[44,45] Recent experimental data demonstrated helical wrapping of SWNTs by poly(para-phenyleneethynylene) (PPES),[39] which resulted in helical pitches of ∼14 nm that correspond to the wrapping angles of ∼17°. By means of scanning tunneling microscopy (STM), it was also observed that the PmPV polymer wraps around nanotubes at ∼19°.[40] Consequently, the geometries of SWNT/PPV hybrids we predicted from MM3 force field optimization are in good agreement with available experimental data. It is important to note that, in experiment, samples are usually being sonicated. Sonication should affect hybrids with very small wrapping angles, since polymers placed parallel to the tube surface can be removed due to the mechanical motion of composites in the solvent, compared to the structures where polymers are helically wrapped around the tube. Therefore, hybrids with vanishing wrapping angles $\alpha \approx 0°$ are usually not detected in experimental measurements.[39,67−69]

**Absorption Spectra of Polymer/SWNTs Hybrids.** In order to estimate the influence of PPV oligomer wrapping on the optical spectrum of PPV−SWNT systems, we performed INDO/S-CIS calculations for three different structures for each type of (6,5)- and (8,0)-hybrids shown in Figure 1. The A2 and B2 structures have been chosen to study the properties of unstable hybrids with long oligomers and large wrapping angles. The A7, A8 and B6, B7 hybrids were chosen to observe effects of relatively strong polymer−tube interactions in hybrids with small wrapping angles of $5° < \alpha < 20°$. In the spectra of all hybrids shown in Figure 3, the strong absorption band at ∼1.6 and ∼1.4 eV for (6,5)- and (8,0)- hybrids, respectively, mainly corresponds to the lowest-energy optically active $E_{11}$ excitonic transition (see Table 2, last column). A very small red-shift of ∼4 meV of this band and an insignificant decrease of its intensity is observed in (6,5)-hybrids compared to the spectra of the isolated (6,5) tube. Such changes are of the order of a standard error value of the corresponding computational methods. However, we notice that PPV more strongly affects the first excitonic band of the (8,0) nanotube: Its intensity is reduced, and its red-shift is ∼15 meV, which slightly increases for stronger-interacting hybrids.

Small red-shifts (≤30 meV) and broadening of the low-energy peak in the absorption spectra of narrow diameter SWNTs upon functionalization by several types of conjugated polymers have been experimentally detected.[39,70] The larger experimental red-shifts, compared to our calculations, can be explained by the solvent effects, which are not included in our calculations, and different types of polymers used in experimental samples. Analysis of the experimental results suggests that the value of the red-shift and degree of broadening of the first band is controlled by the chirality and diameter of the SWNTs, as well as the polymer's chemical structure.[39] This observation is in good agreement with our calculations. The weakness of the overall effect of the PPV functionalization on the $E_{11}$ band of SWNTs has two possible origins. First, due to its very rigid structure, the geometry of the nanotube is insignificantly perturbed by the physisorption of the polymer, resulting in small changes in its optical properties. Second, coupling between nanotube and polymer excited states is minimal; e.g., molecular orbitals contributing to the $E_{11}$ transition are mostly localized on the tube (see NTOs in Figure 5), while orbitals associated with PPV excitations lie much higher in energy and do not noticeably contribute to this transition.

The influence of PPV wrapping is more pronounced on the second excitonic band, $E_{22}$, appearing in the region of ∼2.4 eV for the (6,5) SWNT, as shown in Figure 3. In this hybrid, $E_{22}$ is


dx.doi.org/10.1021/jp211541q | J. Phys. Chem. C 2012, 116, 6831−6840

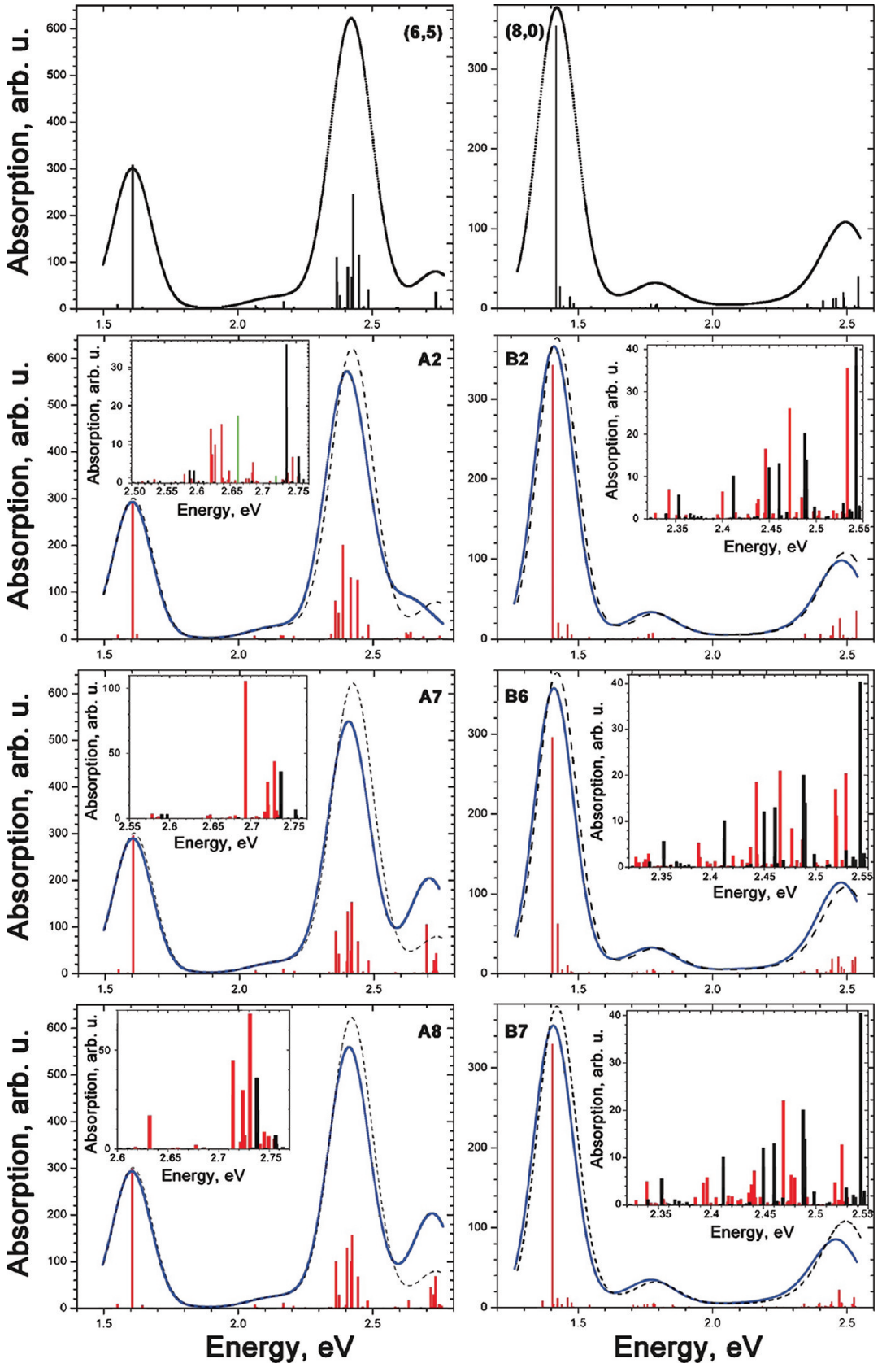


**Figure 3.** Calculated absorption spectra of pristine SWNTs (solid and dashed black lines) and PPV/SWNT composites (solid red and blue lines). Specifically, shown are spectra for pristine (6,5) and (8,0) tubes as well as hybrid A2, B2, A7, B6, A8, and B7 structures. Vertical lines correspond to the oscillator strengths of optical transitions. Insets show optical transitions at the higher energy range. Green vertical lines denote transitions originating from the PPV oligomers.


dx.doi.org/10.1021/jp211541q | J. Phys. Chem. C 2012, 116, 6831−6840

lower in intensity and red-shifted by about 40 meV compared to the $E_{22}$ in the respective isolated tube. This effect is even larger in the energy regions overlapping with polymer excited states. Thus, insets in Figure 3 show the energy range of 2.6–2.8 eV, where broadening and red shifts of the original bands from the pristine SWNT are noticeable, and new optically active states localized on the PPV chain appear (green lines in Figure 3, 1b). Overall, in the interplay between the polymer–SWNT interactions and the energy-resonance of the polymer and nanotube orbitals, the latter has a larger effect on the optical transitions of hybrids. Therefore, we predict that, if low band gap conjugated polymers with optical absorption in the range 1.4–2 eV,[71] such as PDTPBT, are used for SWNT functionalization, the $E_{11}$ band of the nanotube will be much more affected and red-shifted compared to PPV-functionalized SWNTs.

Interestingly, optical transitions associated with the PPV chain appear in the 2.5–2.7 eV spectral window only in the case of the A2 hybrid (Figure 3, 1b), where the PPV oligomer has the most coiled structure and the longest length. It is well-known that an increase of the conjugation length in oligomers red-shifts their vertical transition energies.[72] Figure 4 presents the absorption spectra of the isolated PPV oligomers in their ideal, optimized geometries (planar) and in the configuration they have as hybrids (coiled). As expected, both planar and coiled PPV structures of 17 units in length (A2) have the lowest energy optical transitions (starting at ~2.65 eV), compared to shorter PPV configurations. Therefore, it comes as no surprise that absorption bands related to smaller PPV oligomers in the other hybrids appear at higher energies >2.80 eV (not shown in Figure 3). On the other hand, oligomers with large coiling angles tend to have broader and blue-shifted spectra with slightly lower intensity compared to their linear counterparts, as follows from Figure 4 and Table 2. This blue-shift originates from specific PPV coiling conformations, while the nature of the PPV lowest excited states and their spatial extent on the polymer chain remains the same in both coiled and linear structures (see Tables S2 and S3 in the Supporting Information). To rationalize observed blue-shifts, we recall that the lowest excited state in linear chains gains most of the oscillator strength from the parent excitonic band. In contrast, for chains with coiled geometry, such as those found in our hybrid structures, higher excited states forming complex standing waves on the chain[73–75] become optically allowed due to symmetry reasons leading to constructive and destructive transition dipole interferences between loops, similar to phenomena observed in molecular aggregates with complex geometries.[76,77]

Our calculated results presented in Figure 4 are consistent with experimental data,[78–80] where incorporation of SWNTs in a PPV polymer matrix results in a blue-shift and decrease of the absorption intensity compared to the pristine PPV sample.[81] These modified optical properties have been explained by shortening of the effective $\pi$-conjugation length of PPV chains in the composite due to PPV wrapping around the nanotubes. The morphological structure of such a composite can be represented[79] by a mixture of poorly packed short oligomers and well-packed long oligomers of PPV on the surface of SWNTs. According to our calculations, the appearance of a well-defined broad peak in the range of 3–3.3 eV and a small red-shifted peak at 2.6 eV in coiled PPVs versus one sharp peak at 2.8 eV of the near-linear PPV chains, corresponding to small wrapping angles, could serve as a signature of the helical

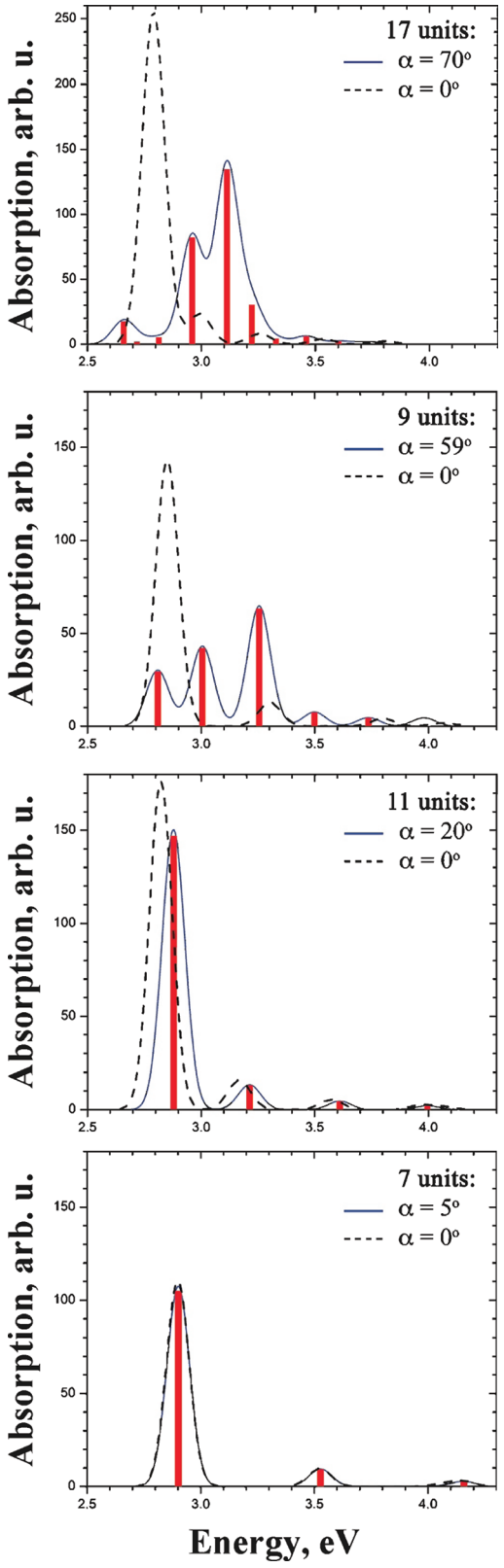


**Figure 4.** Calculated absorption spectra of isolated coiled PPV oligomers (solid red and blue lines) and corresponding linear structures of the PPV chains (dashed black lines). The panels are listed according to decreasing values of wrapping angle (starting from the top): A2-like structure; B2-like structure; A7-like structure; A8-like structure. Red vertical lines correspond to the oscillator strength values of optical transitions.


dx.doi.org/10.1021/jp211541q | J. Phys. Chem. C 2012, 116, 6831–6840

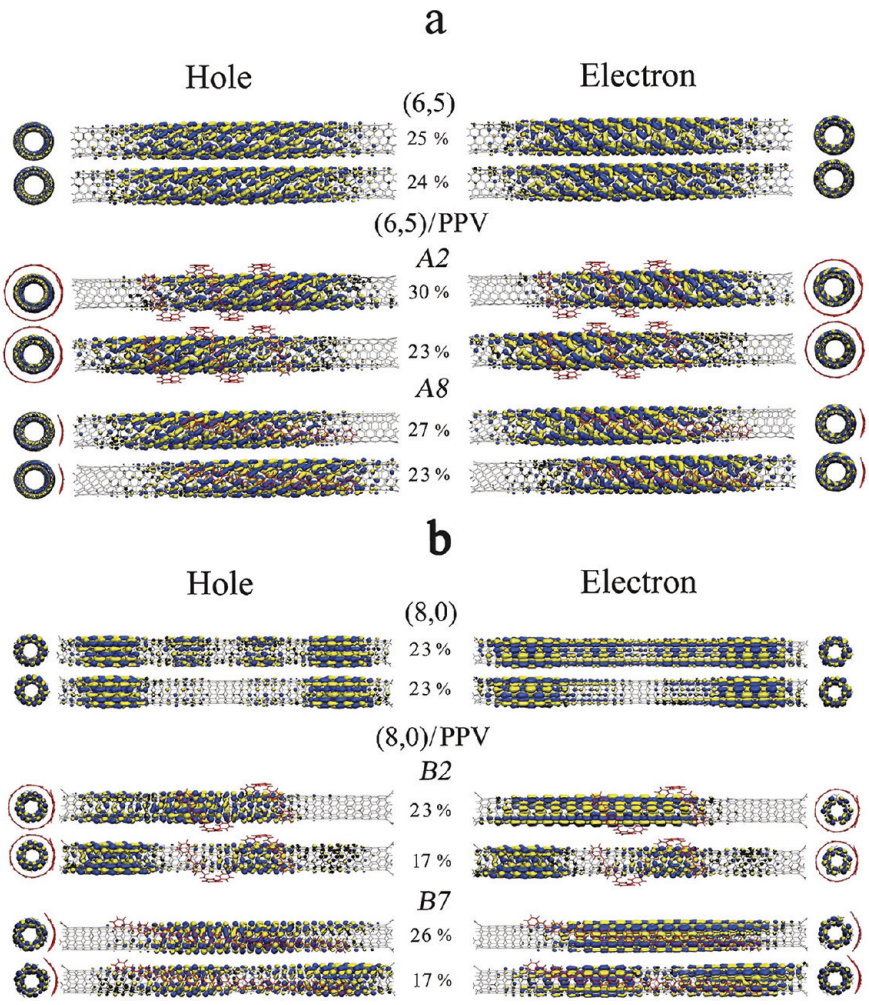


**Figure 5.** Electron and hole natural transition orbitals (NTOs) contributing to the $E_{11}$ electronic transition of the pristine nanotube and selected PPV/SWNT hybrids. The top and bottom panels show (6,5) and (8,0) tubes, respectively. The values between the columns represent the percent of the excited electron−hole density corresponding to the presented NTO. Side and front views of orbitals are displayed using isosurfaces of equal amplitude (0.006).

wrapping of PPV polymers around the nanotube. Thus, these features in the absorption and emission spectra could be useful to detect the dominant structures of the SWNT−polymer hybrids using optical measurements. Analogous signatures of the wrapped versus aligned poly[9,9-dioctylfluorenyl-2,7-diyl] polymers (PFO) associated with red-shifted peak in photoluminescence spectra have been reported in PFO−SWNT hybrids.[49] It was also found[79] that photoluminescence in this composite occurs without contributions from the SWNT network, supporting our results on negligible overlaps between the nanotube excitonic wave functions and polymer orbitals.

**Nature of the Lowest Excited States in PPV/SWNT Hybrids.** In order to analyze the optically active $E_{11}$ transition of SWNTs, we performed NTO analysis for several selected hybrid structures and corresponding isolated SWNTs, as shown in Figure 5. Two dominant pairs of electron and hole NTOs almost equally contribute to the $E_{11}$ transition of the pristine (6,5) and (8,0) nanotubes. In general, electron and hole NTOs for this excitation are delocalized along the tubes. However, the difference in the chirality angle and dimensions of these tubes defines formation of distinct patterns of the NTO orbital "clouds" and the amount of nodes seen. Thus, the electron and hole orbitals of the (6,5) SWNT have larger amplitudes for the central part of the tube and smaller amplitudes for the peripheral sites (Figure 5a), whereas hole NTOs for the (8,0) tube have opposite characteristics with slightly smaller amplitudes located at the center of the tube (Figure 5b).

Similar to the pristine tubes, each dominant NTO pair contributing to the $E_{11}$ transition represents a delocalized $\pi-\pi^*$ character of excitations in SWNT−PPV composites. An amplitude distribution of lower-energy NTOs suggests that the electron and hole are mostly located on the tube with a slightly larger shift of the orbitals toward the ends of the nanotube than it was observed in the pure SWNTs. Compared to the pristine (6,5) tube, rather small changes are seen for electron/hole NTOs of the tube in the corresponding hybrids. In contrast, the almost ideally symmetrical electron/hole NTOs of the (8,0) tube undergo significant asymmetric changes due to PPV functionalization. Such noticeable changes in the NTOs upon PPV wrapping are responsible for stronger red-shifts and decreased intensities in the absorption spectra of (8,0)-PPV hybrids (see Figure 3). The observed difference in NTOs between the (6,5)- and (8,0)-PPV hybrids points on some sensitivity of optical transitions to the tube chirality in polymer-functionnalized SWNTs. Overall, PPV functionalization causes only small perturbations to the low-energy excited electron and


dx.doi.org/10.1021/jp211541q | J. Phys. Chem. C 2012, 116, 6831−6840

Table 2. Calculated Absorption Data for PPV Oligomers and Corresponding PPV/SWNT Hybrids: Transition Energies, eV, and Oscillator Strengths (in Parentheses)

| | first 10 excited states in the absorption spectrum of the isolated coiled PPV oligomer | | | | | | | | | | |
|---|---|---|---|---|---|---|---|---|---|---|---|
| structure | $S_1$ | $S_2$ | $S_3$ | $S_4$ | $S_5$ | $S_6$ | $S_7$ | $S_8$ | $S_9$ | $S_{10}$ | $E_{11}$ exciton in hybrids[a] |
| A2 | 2.66 (0.83) | 2.72 (0.09) | 2.81 (0.25) | 2.96 (3.91) | 3.11 (6.40) | 3.22 (1.44) | 3.33 (0.20) | 3.46 (0.29) | 3.60 (0.11) | 3.73 (0.09) | 1.61 (13.87) |
| A5 | 2.85 (4.30) | 2.96 (0.003) | 3.11 (0.55) | 3.27 (0.003) | 3.44 (0.18) | 3.60 (0.001) | 3.76 (0.09) | 3.92 (0.001) | 4.04 (0.02) | 4.04 (0.01) | 1.60 (14.03) |
| A7 | 2.88 (7.00) | 3.03 (0.00) | 3.21 (0.62) | 3.41 (0.00) | 3.61 (0.21) | 3.81 (0.00) | 3.99 (0.09) | 4.073 (0.00) | 4.074 (0.00) | 4.08 (0.00) | 1.60 (14.09) |
| A8 | 2.90 (5.00) | 3.20 (0.00) | 3.53 (0.44) | 3.85 (0.00) | 4.07 (0.01) | 4.07 (0.00) | 4.07 (0.00) | 4.08 (0.00) | 4.08 (0.00) | 4.16 (0.13) | 1.60 (14.19) |
| B2 | 2.81(1.40) | 3.01 (2.00) | 3.26 (3.01) | 3.50 (0.35) | 3.74 (0.21) | 3.95 (0.03) | 3.98 (0.06) | 3.98 (0.04) | 3.99 (0.03) | 3.99 (0.05) | 1.41 (16.31) |
| B6 | 2.84 (7.37) | 3.02 (0.07) | 3.23 (0.65) | 3.45 (0.01) | 3.68 (0.22) | 3.89 (0.00) | 4.06 (0.01) | 4.07 (0.06) | 4.07 (0.00) | 4.07 (0.00) | 1.40 (14.10) |
| B7 | 2.83 (7.36) | 3.01 (0.04) | 3.23 (0.67) | 3.45 (0.02) | 3.67 (0.22) | 3.89 (0.01) | 4.06 (0.01) | 4.07 (0.06) | 4.07 (0.00) | 4.07 (0.01) | 1.40 (15.72) |

[a]The first optically allowed $E_{11}$ exciton in the spectra of (6,5)-PPV and (8,0)-PPV hybrids corresponds to the fifth ($S_5$) and eleventh ($S_{11}$) transitions, respectively. The transition dipole moment associated with the $E_{11}$ exciton has a dominant $z$-component directed along the tube axis.

hole orbitals of the nanotube; therefore, the effect on the $E_{11}$ excitonic band is insignificant in SWNT−PPV composites.

## CONCLUSIONS

The present study provides a theoretical viewpoint on the relationship between the optical properties of PPV/SWNT composites and their morphological features. Analysis of the (6,5)- and (8,0)-hybrids suggests energetically preferred PPV wrapping at smaller wrapping angles (≤20°) with respect to the tube axis. Our study confirms that PPV oligomers wrapped around the nanotube insignificantly affect the lowest $E_{11}$ absorption band in hybrids, resulting in tiny red-shits, broadening, and a small decrease in the intensity of the $E_{11}$ band. The values of such red-shifts and spectral broadening depend on the chirality of the nanotube. Absorption spectra of hybrids, however, are more affected in the region of higher energies relevant to the $E_{22}$ band, which are close in energy to the excited states of PPV. Our calculations show that the absorption spectra of the nanotubes are almost insensitive to the coiling angle of the PPV chain. In contrast, coiling conformations significantly blue-shift and broaden the absorption spectra of the PPV oligomers, compared to near-linear conformations corresponding to zero or very small wrapping angles. Such blue-shifted features in the absorption and emission spectra of hybrids can be used as signatures of the helical wrapping of the polymer chain around the nanotube to detect the dominant structures of the SWNT−polymer hybrids from optical responses.

## ASSOCIATED CONTENT

### Supporting Information

Structural parameters are listed for isolated PPV oligomers and those in PPV/SWNT hybrids. Transition orbital analysis of lowest excited states of linear and coiled PPV oligomers is also provided. This material is available free of charge via the Internet at http://pubs.acs.org.

## AUTHOR INFORMATION

### Corresponding Author

*E-mail: svetlana.kilina@ndsu.edu.

### Notes

The authors declare no competing financial interest.

## ACKNOWLEDGMENTS

S.V.K. acknowledges financial support from ND EPSCoR NSF grant no. EPS-0814442 and NIH COBRE grant P20PR015566. A.F. and J.L. acknowledge financial support from MS EPSCoR NSF grant no. 362492-190200-01\NSFEPS-0903787. S.V.K. and A.F. thank Ekaterina Badaeva for the fruitful discussions. S.V.K. thanks David Hogle and Michael Mayo for the help with the manuscript. We also acknowledge support of Center for Integrated Nanotechnology (CINT), Center for Nonlinear Studies (CNLS), and the LDRD program at Los Alamos National Laboratory, operated by Los Alamos National Security, LLC, for the National Nuclear Security Administration of the U.S. Department of Energy under contract DE- AC52-06NA25396.

## REFERENCES

(1) Usmani, F. A.; Hasan, M. *Microelectron. J.* **2010**, *41*, 395−402.
(2) Wind, S. J.; Appenzeller, J.; Avouris, P. *Phys. Rev. Lett.* **2003**, *91*, 583011−583014.
(3) Javey, A.; Guo, J.; Wang, Q.; Lundstrom, M.; Dai, H. *Nature* **2003**, *424*, 654−657.
(4) Lefebvre, J.; Homma, Y.; Finnie, P. *Phys. Rev. Lett.* **2003**, *90*, 2174011−2174014.

(5) Bachilo, S. M.; Strano, M. S.; Kittrell, C.; Hauge, R. H.; Smalley, R. E.; Weisman, R. B. *Science* **2002**, *298*, 2361−2366.
(6) Barazzouk, S.; Hotchandani, S.; Vinodgopal, K.; Kamat, P. V. *J. Phys. Chem. B* **2004**, *108* (44), 17015−17018.
(7) Byon, H. R.; Choi, H. C. *J. Am. Chem. Soc.* **2006**, *128*, 2188−2189.
(8) Star, A.; Tu, E.; Niemann, J.; Gabriel, J. C. P.; Joiner, C. S.; Valcke, C. *Proc. Natl. Acad. Sci. U.S.A.* **2006**, *103*, 921−926.
(9) Patolsky, F.; Zheng, G. F.; Hayden, O.; Lakadamyali, M.; Zhuang, X. W.; Lieber, C. M. *Proc. Natl. Acad. Sci. U.S.A.* **2004**, *101*, 14017−14022.
(10) Tang, B. Z.; Xu, H. Y. *Macromolecules* **1999**, *32*, 2569−2576.
(11) O'Connell, M. J.; Boul, P.; Ericson, L. M.; Huffman, C.; Wang, Y.; Haroz, E.; Kuper, C.; Tour, J.; Ausman, K. D.; Smalley, R. E. *Chem. Phys. Lett.* **2001**, *342*, 265−271.
(12) Star, A.; Steuerman, D. W.; Heath, J. R.; Stoddart, J. F. *Angew. Chem., Int. Ed.* **2002**, *41*, 2508−2512.
(13) Star, A.; Gabriel, J. C. P.; Bradley, K.; Gruner, G. *Nano Lett.* **2003**, *3*, 459−463.
(14) Zheng, M.; Jagota, A.; Semke, E. D.; Diner, B. A.; McLean, R. S.; Lustig, S. R.; Richardson, R. E.; Tassi, N. G. *Nat. Mater.* **2003**, *2*, 338−342.
(15) Curran, S. A.; Ajayan, P. M.; Blau, W. J.; Carroll, D. L.; Coleman, J. N.; Dalton, A. B.; Davey, A. P.; A. Drury, B. M.; Maier, S.; Strevens, A. *Adv. Mater.* **1998**, *10*, 1091−1093.
(16) Keogh, S. M.; Hedderman, T. G.; Lynch, P.; Farrell, G. F.; Byrne, H. J. *J. Phys. Chem. B* **2006**, *110*, 19369−19374.
(17) Coleman, J. N.; Curran, S.; Dalton, A. B.; Davey, A. P.; McCarthy, B.; Blau, W.; Barklie, R. C. *Phys. Rev. B* **1998**, *58*, R7492−R7495.
(18) Coleman, J. N.; Curran, S.; Dalton, A. B.; Davey, A. P.; Mc Carthy, B.; Blau, W.; Barklie, R. C. *Synth. Met.* **1999**, *102*, 1174−1175.
(19) Park, C.; Ounaies, Z.; Watson, K. A.; Crooks, R. E.; Smith, J.; Lowther, S. E.; Connell, J. W.; Siochi, E. J.; Harrison, J. S.; Clair, T. L. S. *Chem. Phys. Lett.* **2002**, *364*, 303−308.
(20) Pinto, N. J.; Johnson, A. T.; MacDiarmid, A. G.; Mueller, C. H.; Theofylaktos, N.; Robinson, D. C.; Miranda, F. A. *Appl. Phys. Lett.* **2003**, *83*, 4244−4246.
(21) Freitag, M.; Martin, Y.; Misewich, J. A.; Martel, R.; Avouris, P. H. *Nano Lett.* **2003**, *3*, 1067−1071.
(22) Dalton, A. B.; Stephan, C.; Coleman, J. N.; McCarthy, B.; Ajayan, P. M.; Lefrant, S.; Bernier, P.; Blau, W. J.; Byrne, H. J. *J. Phys. Chem. B* **2000**, *104*, 10012−10016.
(23) Panhuis, M.; Maiti, A.; Dalton, A. B.; Noort, A. V. D.; Coleman, J. N.; McCarthy, B.; Blau, W. J. *J. Phys. Chem. B* **2003**, *107*, 478−482.
(24) Lemasson, F. A.; Strunk, T.; Gerstel, P.; Hennrich, F.; Lebedkin, S.; Barner-Kowollik, C.; Wenzel, W.; Kappes, M. M.; Mayor, M. *J. Am. Chem. Soc.* **2011**, *133*, 652−655.
(25) Ozawa, H.; Fujigaya, T.; Niidome, Y.; Hotta, N.; Fujiki, M.; Nakashima, N. *J. Am. Chem. Soc.* **2011**, *133*, 2651−2657.
(26) Tange, M.; Okazaki, T.; Iijima, S. *J. Am. Chem. Soc.* **2011**, *133*, 11908−11911.
(27) Steuerman, D. W.; Star, A.; Narizzano, R.; Choi, H.; Ries, R. S.; Nicolini, C.; Stoddart, J. F.; Heath, J. R. *J. Phys. Chem. B* **2002**, *106*, 3124−3130.
(28) Mallajosyula, A. T.; Iyer, S.; Mazhari, B. *J. Appl. Phys.* **2010**, *108*, 094902−9.
(29) Stranks, S.; Weisspfennig, C.; Parkinson, P.; Johnston, M.; Herz, L.; Nicholas, R. *Nano Lett.* **2011**, *11*, 66−72.
(30) Dalton, A.; Chambers, G.; Byrne, H.; Coleman, J.; McCarthy, B.; Panhuis, M.; Blau, W.; Duesburg, G.; Roth, S.; Ajayan, P. *Recent Res. Dev. Phys. Chem.* **2002**, *6*, 327−349.
(31) Curran, S.; Dalton, A.; Davey, A.; McCarthy, B.; Blau, W.; Barklie, R. *Phys. Rev. B* **1998**, *58*, R7492−R7495.
(32) Benoit, J.; Corraze, B.; Lefrant, S.; Blau, W.; Bernier, P.; Chauvet, O. *Synth. Met.* **2001**, *121*, 1215−1216.
(33) Aarab, H.; Baitoul, M.; Wery, J.; Almairac, R.; Lefrant, S.; Faulques, E.; Duvail, J.; Hamedounb, M. *Synth. Met.* **2005**, *155*, 63−67.
(34) Singh, I.; Madhwal, D.; Verma, A.; Kumar, A.; Rait, S.; Kaur, I.; Bharadwaj, L.; Bhatia, C.; Bhatnagar, P.; Mathur, P. *J. Lumin.* **2010**, *130*, 2157−2160.
(35) Lee, K. W.; Lee, S. P.; Choi, H.; Mo, K. H.; Jang, J. W.; Kweon, H.; Lee, C. E. *Appl. Phys. Lett.* **2007**, *91*, 023110−1−4.
(36) Gao, J.; Loi, M. A. *Eur. Phys. J. B* **2010**, *75*, 121−126.
(37) Jiang, L. Y.; Huang, Y.; Jiang, H.; Ravichandran, G.; Gao, H.; Hwang, K. C.; Liu, B. J. *J. Mech. Phys. Solids* **2006**, *54*, 2436−2452.
(38) Chen, R. J.; Zhang, Y.; Wang, D.; Dai, H. *J. Am. Chem. Soc.* **2001**, *123*, 3838−3839.
(39) Kang, Y. K.; Lee, O.-L.; Deria, S. H.; Kim, T.-H.; Park, D. A.; Bonnell, J. G.; Saven.; Therien, M. J. *Nano Lett.* **2009**, *9*, 1414−1418.
(40) Carthy, B. M.; Coleman, J.; Czerw, R.; Dalton, A.; Panhuis, M.; Maiti, A.; Drury, A.; Byrne, H.; Carroll, D.; Blau, W. *J. Phys. Chem. B* **2002**, *106*, 2210−2216.
(41) Collison, C.; Spencer, S.; Preske, A.; Palumbo, C.; Helenic, A.; Bailey, R.; Pellizzeri, S. *J. Phys. Chem. B* **2010**, *114*, 11002−11009.
(42) Chen, J.; Liu, H. Y.; Weimer, W. A.; Halls, M. D.; Waldeck, D. H.; Walker, G. C. *J. Am. Chem. Soc.* **2002**, *124*, 9034−9035.
(43) Holt, J.; Ferguson, A.; Kopidakis, N.; Larsen, B.; Bult, J.; Rumbles, G.; Blackburn, J. *Nano Lett.* **2010**, *10*, 4627−4633.
(44) Tallury, S. S.; Pasquinelli, M. A. *J. Phys. Chem. B* **2010**, *114*, 9349−9355.
(45) Tallury, S. S.; Pasquinelli, M. A. *J. Phys. Chem. B* **2010**, *114*, 4122−4129.
(46) Caddeo, C.; Melis, C.; Colombo, L.; Mattoni, A. *J. Phys. Chem. C* **2010**, *114*, 21109−21113.
(47) Liu, Y.; Chipot, C.; Shao, X.; Cai, W. *J. Phys. Chem. C* **2011**, *115*, 1851−1856.
(48) Gurevitch, I.; Srebnik, S. *Chem. Phys. Lett.* **2007**, *444*, 96−100.
(49) Gao, J.; Loi, M. A.; de Carvalho, E. J.; dos Santos, M. C. *ACS Nano* **2011**, *5*, 3993−3999.
(50) Yang, M.; Koutsos, V.; Zaiser, M. *J. Phys. Chem. B* **2005**, *109*, 10009−10014.
(51) Dewar, M. J. S.; Zoebisch, E. G.; Healy, E. F.; Stewart, J. J. P. *J. Am. Chem. Soc.* **1985**, *107*, 3902−3909.
(52) Kilina, S.; Tretiak, S. *Adv. Funct. Mater.* **2007**, *17*, 3405−3420.
(53) Tretiak, S. *Nano Lett.* **2007**, *7*, 2201−2206.
(54) Tretiak, S.; Kilina, S.; Piryatinski, A.; Saxena, A.; Martin, R. L.; Bishop, A. R. *Nano Lett.* **2007**, *7*, 86−92.
(55) Kilina, S.; Badaeva, E.; Piryatinski, A.; Tretiak, S.; Saxena, A.; Bishop, A. R. *Phys. Chem. Chem. Phys.* **2009**, *11*, 4113−4123.
(56) Ponder, J. W. http://dasher.wustl.edu/tinker, 2004.
(57) Allinger, N. L.; Yuh, Y. H.; Lii, J. H. *J. Am. Chem. Soc.* **1989**, *111*, 8551−8566.
(58) Lii, J. H.; Allinger, N. L. *J. Comput. Chem.* **1998**, *19*, 1001−1016.
(59) Yang, P.; Batista, E. R.; Tretiak, S.; Saxena, A.; Martin, R. L.; Smith, D. L. *Phys. Rev. B* **2007**, *76*, 241201.
(60) Kilina, S.; Batista, E. R.; Yang, P.; Tretiak, S.; Saxena, A.; Martin, R. L.; Smith, D. L. *ACS Nano* **2008**, *2*, 1381−1388.
(61) Mukamel, S.; Tretiak, S.; Wagersreiter, T.; Chernyak, V. *Science* **1997**, *277*, 781.
(62) Tretiak, S.; Mukamel, S. *Chem. Rev.* **2002**, *102* (9), 3171−3212.
(63) Chernyak, V.; Schulz, M. F.; Mukamel, S.; Tretiak, S.; Tsiper, E. V. *J. Chem. Phys.* **2000**, *113*, 36−43.
(64) Martin, R. L. *J. Chem. Phys.* **2003**, *118*, 4775−4777.
(65) Frisch, M. J.; et al. *Gaussian 03*; Gaussian, Inc.: Wallingford, CT, 2009.
(66) Sinnokrot, M. O.; Valeev, E. F.; Sherrill, C. D. *J. Am. Chem. Soc.* **2002**, *124*, 10887−10893.
(67) Saini, V.; Li, Z.; Bourdo, S.; Dervishi, E.; Xu, Y.; Ma, X.; Kunets, V.; Salamo, G.; Viswanathan, T.; Biris, A.; Saini, D.; Biris, A. *J. Phys. Chem. C* **2009**, *113*, 8023−8029.
(68) Giulianini, M.; Waclawik, E. R.; Bell, J. M.; Scarselli, M.; Castrucci, P.; Crescenzi, M. D.; Motta, N. *Appl. Phys. Lett.* **2009**, *95*, 143116.
(69) Giulianini, M.; Waclawik, E. R.; Bell, J. M.; Scarselli, M.; Castrucci, P.; Scarselli, M.; Motta, N. *Appl. Phys. Lett.* **2009**, *95*, 013304.

(70) Lüer, L.; Hoseinkhani, S.; Meneghetti, M.; Lanzani, G. *Phys. Rev. B* **2010**, *81*, 155411.
(71) Yue, W.; Zhao, Y.; Shao, S.; Tian, H.; Xie, Z.; Geng, Y.; Wang, F. *J. Mater. Chem.* **2009**, *19*, 2199−2206.
(72) Hennebicq, E.; Pourtois, G.; Scholes, G. D.; Herz, L. M.; Russell, D. M.; Silva, C.; Setayesh, S.; Grimsdale, A. C.; Mullen., K; Bredas, J.-L.; Beljonne, D. *J. Am. Chem. Soc.* **2005**, *127*, 4744−4762.
(73) Wu, C.; Malinin, S. V.; Tretiak, S.; Chernyak, V. Y. *Phys. Rev. Lett.* **2008**, *100*, 057405.
(74) Wu, C.; Malinin, S. V.; Tretiak, S.; Chernyak, V. Y. *Nat. Phys.* **2006**, *2*, 631−635.
(75) Tretiak, S.; Igumenshchev, K.; Chernyak, V. *Phys. Rev. B* **2005**, *71*, 33201.
(76) Tretiak, S.; Zhang, W. M.; Chernyak, V.; Mukamel, S. *Proc. Natl. Acad. Sci. U.S.A.* **1999**, *96*, 13003−13008.
(77) Katan, C.; Tretiak, S.; Werts, M. H. V.; Bain, A. J.; Marsh, R. J.; Leonczek, N.; Nicolaou, N.; Badaeva, E.; Mongin, O.; Blanchard-Desce, M. *J. Phys. Chem. B* **2007**, *111*, 9468−9483.
(78) Mulazzi, E.; Perego, R.; Aarab, H.; Mihut, L.; Lefrant, S.; Faulques, E.; Wery, J. *Phys. Rev. B* **2004**, *70*, 155206−1−9.
(79) Mulazzi, E.; Perego, R.; Wery, J.; Mihut, L.; Lefrant, S.; Faulques, E. *J. Chem. Phys.* **2006**, *125*, 014703.
(80) Curran, S.; Davey, A. P.; Coleman, J.; Dalton, A.; McCarthy, B.; Maier, S.; Drury, A.; Gray, D.; Brennan, M.; Ryder, K.; Chapelle, M. L. D. L.; Journet, C.; Bernier, P.; Byrne, H. J.; Carroll, D.; Ajayan, P. M.; Lefrant, S.; Blau, W. *Synth. Met.* **1999**, *103*, 2559−2562.
(81) Mulazzi, E.; Ripamonti, A.; Wery, J.; Dulieu, B.; Lefrant, S. *Phys. Rev. B* **1999**, *60*, 16519−16525.